Cation Site and Anion Charge Ordering in Body-Centered Cubic-Packed Fullerides with Complex Counterions

J. B. Claridge,* A. J. Fowkes, M. J. Rosseinsky,* and I. D. Watts

Department of Chemistry, University of Liverpool, Liverpool, L69 7ZD, U.K.

Received January 2, 2002. Revised Manuscript Received January 2, 2003

Two fullerides derived from Na_2C_{60} by ammonia coordination to the counterions are presented. Both structures adopt body-centered cubic-related anion packings. The sodium cations are extensively disordered in one phase, but their positional ordering in the second phase is correlated with the development of two distinct fulleride anion environments. Electrostatic considerations indicate that the two crystallographically distinct fulleride anions display charge separation.

Introduction

The formation of complex counterions in fullerides by coordination of ammonia to intercalated metal cations has proved a versatile technique both for the expansion of fcc A_3C_{60} phases and the synthesis of novel fulleride structures.[1] The resulting expansion of the fulleride array can result in new electronic ground states, such as magnetic ordering in ammoniated $(NH_3)A_3C_{60}$[2,3] phases, which demonstrates the importance of electron correlation in the narrow band fullerides. Na_2C_{60} has previously been reported to afford rhombohedral $(ND_3)_8$-Na_2C_{60} and a body-centered cubic (bcc)-related $(NH_3)_{5.3}$-Na_2C_{60} phase.[4] In this paper we determine the structures of two bcc-packed ammoniated fullerides closely related to $(ND_3)_{5.3}Na_2C_{60}$, which differ in that occupancy of the interstitial cation sites is ordered in one case and disordered in the other. The cation site ordering, which is driven by the exceptional level of positional disorder found in the disordered phase, is accompanied by the development of two distinct fulleride anion environments. This is consistent with the formation of a charge-ordered array in which the crystallographically distinct anions carry different charges. In view of the importance of such valency ordering in controlling the electronic properties of oxides, and the increasing indications that fullerides are strongly correlated electronic systems, this is an important observation and further reinforces the important role of ammonia coordination to metal cations in discovering new fulleride ground states.

As is common in fulleride science, both structures were determined from powder diffraction data from heavily disordered materials. Both structures are based on body-centered cubic (bcc) anion arrays in which there are six pseudo-tetrahedral interstitial sites per fulleride which are occupied by ammonia molecules. This results in many possible locations for two metal cations (the most favorable sites, occupied in $(NH_3)_6Na_3C_{60}$,[5,6] would accommodate twelve sodium cations per formula unit if fully occupied) and extensive positional disorder. In this paper we show that ordering of the cations over these interstitial sites is possible, but solution of the resulting structure using conventional diffraction methods proves challenging. One method of overcoming this problem is the application of maximum entropy methods (MEM).[7−10] In this approach, rather than performing a Fourier transformation of the F_{obs} structure factors as obtained from the Rietveld refinement by apportioning the intensity of overlapping observed reflections according to the calculated structure factors, a density distribution is estimated and the information entropy contained in the structure factors is maximized within the errors of the observed data. Thus, MEM can be seen in some ways as the opposite of a Fourier synthesis, as an initial density is fitted to the observed structure factors (it is customary to start from a homogeneous density distribution). As unobserved high Q ($Q = 2\pi/d$) peaks therefore do not effect the density, accurate electron densities can be obtained from limited numbers of integrated intensities.[10] The use of MEM alone still maintains the F_{obs} as obtained from the initial extraction and is therefore biased toward the model used to extract the data. The results of an MEM calculation can, however, be used to provide F_{calc} for a second extraction, which will be less biased by the original model. Repeated extractions and MEM calculations should therefore yield the true scattering density. This cycling of the MEM results has been implemented by Izumi in RIETAN-2000 who has applied the REMEDY cycles to a number of diffraction problems.[11,12]

(1) Rosseinsky, M. J. *Chem. Mater.* **1998**, *10*, 2665−2685.
(2) Prassides, K.; Margadonna, S.; Arcon, D.; Lappas, A.; Shimoda, H.; Iwasa, Y. *J. Am. Chem. Soc.* **1999**, *121*, 11227−11228.
(3) Takenobu, T.; Muro, T.; Iwasa, Y.; Mitani, T. *Phys. Rev. Lett.* **2000**, *85*, 381.
(4) Fowkes, A. J.; Fox, J. M.; Henry, P. F.; Heyes, S. J.; Rosseinsky, M. J. *J. Am. Chem. Soc.* **1997**, *119*, 10413.
(5) Henry, P. F.; Rosseinsky, M. J.; Watt, C. J. *J. Chem. Soc., Chem. Commun.* **1995**, 2131−2132.
(6) Fullagar, W. K.; Reynolds, P. A.; White, J. W. *Solid State Commun.* **1997**, *104*, 23.
(7) Collins, D. M. *Nature* **1982**, *298*, 49−51.
(8) Collins, D. M. *Z. Naturforsch., A: Phys. Sci.* **1993**, *48*, 68−74.
(9) Sakata, M.; Mori, R.; Kumazawa, S.; Takata, M.; Toraya, H. *J. Appl. Crystallogr.* **1990**, *23*, 526−534.
(10) Takata, M.; Nishibori, E.; Sakata, M. *Z. Kristallogr.* **2001**, *216*, 71−86.

10.1021/cm020161x CCC: $25.00
Published on Web 03/13/2003

Table 1. Refined Positional Parameters of $(ND_3)_6Na_2C_{60}$ in Space Group *Im* $\bar{3}$ (number 204) (*a* =12.151(3) Å)

name	*x*	*y*	*z*	100 U/Å^2	fractional occupancy	site
C1	0.05667(40)	0.000000	0.28850(32)	4.3 (2)	1	24g
C2	0.11788(21)	0.09844(27)	0.25287(24)	4.9 (1)	1	48h
C3	0.05696(19)	0.18544(23)	0.21382(22)	5.6(1) 1	1	48h
Na4	0.31978(33)	0.34151(29)	0.000000	10.(4)	0.166	24g
N5	0.500000	0.2837(7)	0.000000	8.2(2)	1	12e
D7	0.5589(13)	0.2241(14)	0.0341(7)	13.9(6)	0.25	48h
D8	0.4500(12)	0.3283(13)	0.0608(9)	13.9(6)	0.25	48h
D9	0.4560(15)	0.2567(14)	−0.0743(12)	13.9(6)	0.25	48h

Experimental Section

$(ND_3)_6Na_2C_{60}$ was prepared from $(ND_3)_8Na_2C_{60}$ (synthesized as described in ref 4[4]) by equilibration of the initial $(ND_3)_8Na_2C_{60}$ phase with 0.05 atm of ND_3 vapor at 100 °C. $(NH_3)_{5.3}Na_2C_{60}$ was prepared as described previously[4] by equilibration of Na_2C_{60} with ammonia gas. The composition was determined volumetrically. Neutron powder diffraction data on $(ND_3)_6Na_2C_{60}$ were collected at ambient temperature on the POLARIS powder diffractometer[13] at the ISIS spallation neutron source. The relevant neutron scattering lengths are C = 0.665, D = 0.667, N = 0.930, and Na = 0.363 × 10^{-12} cm. Synchrotron X-ray powder diffraction data were recorded at ambient temperature at station 9.1 of the Daresbury Synchrotron Radiation Source. Data analysis was performed using the GSAS refinement and REMEDY (a combination of RIETAN-2000[12] and MEED[9]) maximum entropy analysis packages. Room temperature ^{13}C MAS NMR data were recorded on $(NH_3)_{5.3}Na_2C_{60}$ on a Bruker MSL200-S NMR spectrometer with an Oxford Instruments 4.7 T wide bore (98 mm) superconducting solenoid magnet equipped with an Aspect 2000 data system. Spectra were recorded at 50.32 MHz using a Bruker Z32 HB-WB-73A MAS7DB probe. All samples for MAS NMR were packed into 5-mm Kel-F capped inserts which were placed into 7-mm zirconia rotors with Kel-F caps − this produced an airtight seal. The spinning speed was 4.2 kHz, and the recycle delay was 20 s.

Results

The ammonia sorption isotherms of Na_2C_{60} display considerable hysteresis, and this is reflected in the subtle structural differences between the two phases discussed here. Both phases give X-ray powder patterns which can be predominantly indexed with the bcc unit cell of $(NH_3)_6Na_3C_{60}$, but differ in that $(NH_3)_{5.3}Na_2C_{60}$ (prepared directly from Na_2C_{60}) displays superstructure reflections characteristic of a primitive trigonal superstructure derived from a trigonal distortion of the bcc subcell adopted by $(ND_3)_6Na_2C_{60}$, prepared by deammoniation of $(ND_3)_8Na_2C_{60}$. We discuss the structure of $(ND_3)_6Na_2C_{60}$ derived by neutron powder diffraction initially because it is the disordered precursor of the ordered $(NH_3)_{5.3}Na_2C_{60}$. Le Bail extraction of the 3 banks of neutron data converged smoothly to $\chi^2 = 2.53$. Analysis of the room-temperature diffraction pattern began with the $(NH_3)_6Na_3C_{60}$ model:[5,6] refinement of the N and Na fractional occupancies indicated that the N site was fully occupied, corresponding to a composition $(ND_3)_6Na_2C_{60}$, and thus the site occupancies were fixed at the values determined by this composition in the subsequent analysis. Difference Fourier analysis to locate the D positions did not yield discrete well-defined maxima, ascribable to the orientational disorder evidenced in the diffraction pattern in which Bragg peaks are not discernible below 1.2 Å. Data collected at 5 K indicate that this positional disorder becomes frozen-in on cooling. A rigid body (initial geometry N−D = 1.12 Å, D−N−D = 109°) model was therefore used to describe the deuterium positions in this phase. Location of the rigid body ND_3 molecules on the *12e* ($^1/_2$, *y*, 0) special positions and difference Fourier analysis lead to the location of Na on *24g* (*x*, *y*, 0) as in $(NH_3)_6Na_3C_{60}$. Both refinement and analysis of difference Fourier maps indicated that there was no N within the vicinity of this site. Refinement of the rigid body rotation angles, N−D bond length and D−N−D angle, site occupancy factors, displacement parameters, and positional parameters for non-ND_3 atoms lead to the model presented in Table 1 and the fit shown in Figure 1. The structure is shown in Figure 2a (The ORTEP representation is provided in Figure S1 of the Supporting Information). The χ^2 value of 2.7 is acceptably close to the Le Bail extraction, indicating that the remaining inadequacies are due to difficulties in describing the peak shape. Well-determined bond-distances and angles are given in Table 2. Refinement in space group $Im\bar{3}m$, in which the C_{60} anion positions are disordered over two orientations related by 90° rotation about [001], was unstable and did not converge below $\chi^2 = 5.0$.

Table 2. Bond Lengths (Å) and Angles (°) in $(ND_3)_6Na_2C_{60}$ Refined from Neutron Powder Diffraction

C1−C1 (×6)	1.38(1)
C2−C3 (×24)	1.375(3)
C1−C2 (×24)	1.474(5)
C2−C3 (×24)	1.511(4)
C3−C3(×12)	1.384(5)
C1−C1−C2 (×2)	120.3(2)
C2−C1−C2	108.5(4)
C1−C2−C3	117.0(3)
C1−C2−C3	106.1(3)
C3−C2−C3	118.9(3)
C2−C3−C2	120.2(3)
C2−C3−C3	122.6(2)
C2−C3−C3	109.5(2)
Na4−N5	2.299(2)
Na4−N5	2.300(5)
N5−Na4−N5	140.9(3)
N5−D7	1.099(5)
D7−N5−D8	115.5(6)

The C_{60}^{2-} anions adopt $m\bar{3}$ symmetry standard orientations in the bcc array. The ND_3 molecules are orientationally disordered within distorted tetrahedral sites in this C_{60}^{2-} array (Figure 2a), with closest C−D contacts of 2.674 Å (C1−D3) and 2.57 Å (C2−D2) (as represented in Figure S2 of the Supporting Information) and several other contacts closer than 2.95 Å seen in solid benzene. This is indicative of N−D...π interactions playing a role in determining the orientation of the ND_3

(11) Izumi, F.; Ikeda, T.; Sasaki, T.; Kumazawa, S. *Mol. Cryst. Liq. Cryst.* **2000**, *341*, 1057−1062.
(12) Izumi, F.; Ikeda, T. *A Rietveld-Analysis Program RIETAN-98 and its Applications to Zeolites*, 2000; Vol. 321-3, pp 198−203.
(13) Hull, S.; Smith, R. I.; David, W. I. F.; Hannon, A. C.; Mayers, J.; Cywinski, R. *Physica B* **1992**, *180 & 181*, 1000−1002.

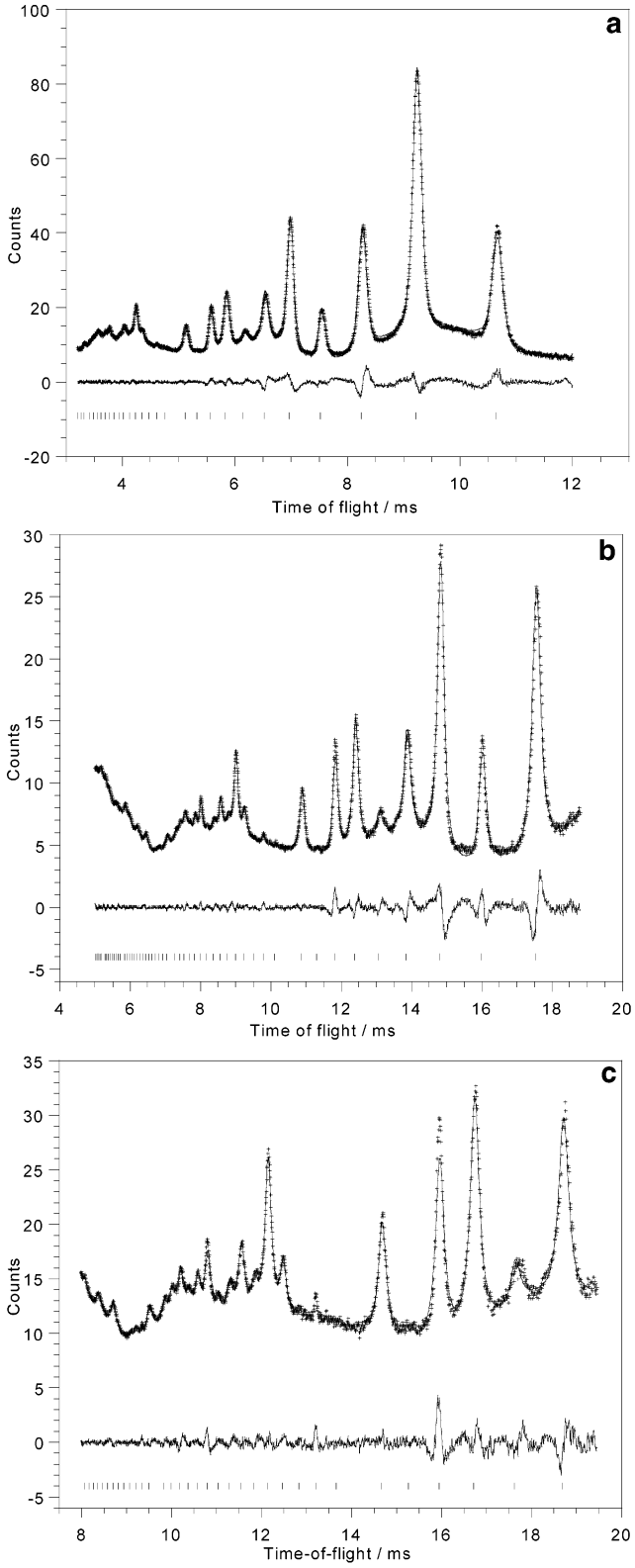

Figure 1. Rietveld fit to time-of-flight neutron powder diffraction data from $(ND_3)_6Na_2C_{60}$. (a) 35° detector bank (1.49 ≤ *d*/ Å ≤ 5.6) (b) 90° detector bank (1.1 ≤ *d*/ Å ≤ 4) (c) 145° detector bank (1.29 ≤ *d*/ Å ≤ 3.2). The observed data are shown as points, the calculated fit is the solid line, and the difference is plotted below. The tick marks indicate the location of the Bragg peaks. $\chi^2 = 2.71$ (86 variables, 7071 data points) for the fit to all three data banks simultaneously. The agreement indices for the individual banks are as follows: 35° $R_w = 4.09\%$, $R(F^2) = 1.88\%$ for 107 reflections; 90° $R_w = 2.47\%$, $R(F^2) = 2.47\%$ for 263 reflections; 145° $R_w = 2.52\%$ $R(F^2) = 0.96\%$ for 154 reflections. The refined parameters are given in Table 1.

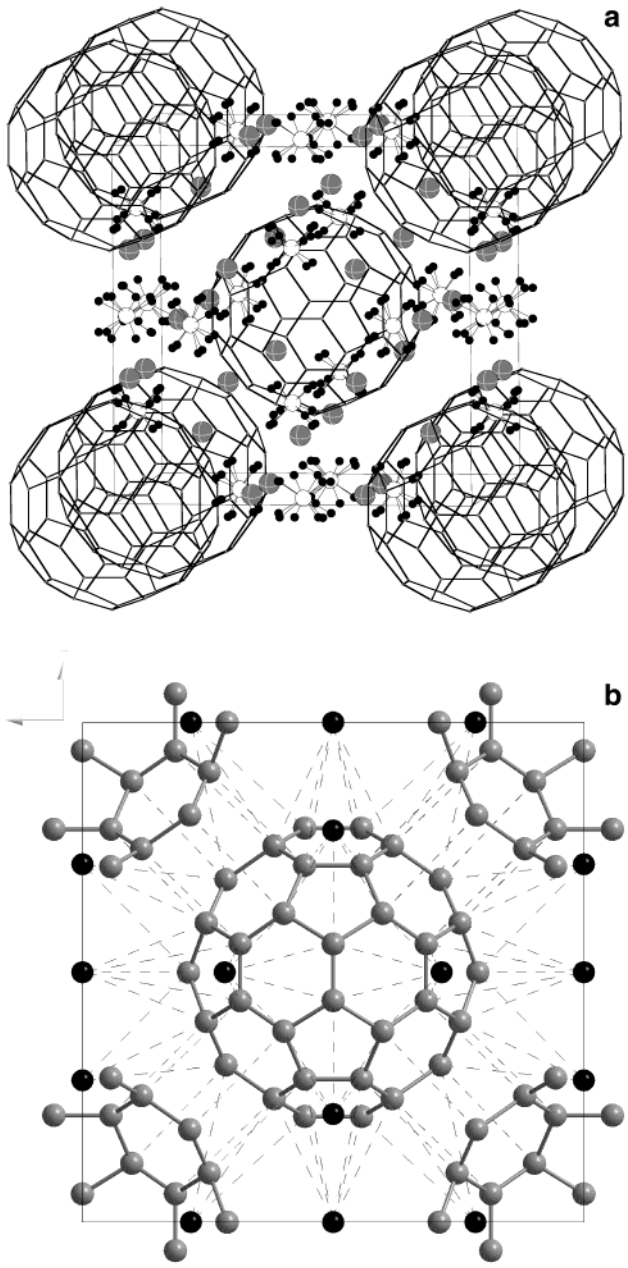

Figure 2. (a) Refined structure of $(ND_3)_6Na_2C_{60}$ (N unshaded, D black, Na gray crossed spheres). The Na sites are $^1/_6$ occupied and thus the structure is considerably positionally disordered. (b) The environment of a C_{60}^{2-} anion in $(ND_3)_6Na_2C_{60}$ defined by contacts to the ND_3 molecules and eight neighboring C_{60}^{2-} anions along the ⟨111⟩ directions, which cap the eight hexagonal faces not involved in ND_3-C_{60} interactions.

units. Each C_{60} is surrounded by 24 ND_3 units: of the 32 faces, all 12 pentagonal, and 12 of the 20 hexagonal faces are capped with ND_3 molecules. The eight fulleride neighbors of a given C_{60}^{2-} anion are located 10.52 Å away along the body diagonals of a cube, and the remaining eight hexagonal faces of the anion are aligned with these directions, remaining uncapped by ammonia molecules (Figure 2b). The close C−D contacts arise from ND_3 neighbors located over hexagonal faces, and allow the ND_3 molecules to link the C_{60}^{2-} anions via these interactions, as the close C...D2 and C...D3 contacts for a given ND_3 are to neighboring anions. None of the D atoms are located over hexagon or pentagon centroids as in $(ND_3)_8Na_2C_{60}$,[4] and this may account for

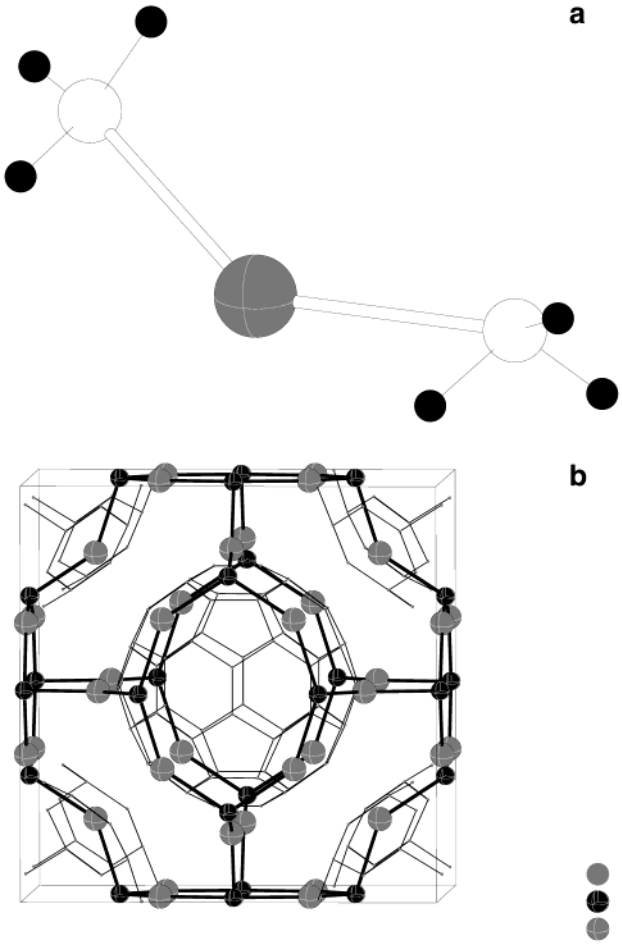

Figure 3. (a) Coordination environment of the Na^+ cations in $(ND_3)_6Na_2C_{60}$. The partial occupancy of the cation sites and orientational disorder of the anion means that other local cation environments are possible. The D atoms are in black, N are unshaded, and Na are gray crosses. (b) The extended network of contacts between the fully occupied ND_3 (dark crossed spheres) sites and the $^1/_6$ occupied Na sites (grey crossed spheres). As each ND_3 makes only four contacts to Na sites (Figure S3 in the Supporting Information), there are ND_3 molecules which do not coordinate to Na^+.

the absence of orientational ordering of the ammonia molecules in the present case.

The $(ND_3)_2Na^+$ complexes (Figure 3) refine with an N−Na−N angle of 140.9(3)°; the Na−C3 contact of 2.356(5) Å is shorter than the radius sum of 2.7 Å and there may be local relaxation of the anion orientation in the vicinity of the 14% occupied Na site. As a result, C3 has the largest displacement parameter of any of the C atoms. The ND_3 site is located equidistant from four partially ($\bar{3}$) occupied Na sites, and the D positions thus represent an average over four possible orientations of the ND_3 unit, together with ND_3 molecules uncoordinated to Na cations (such NH_3 species are observed in the structures of $Ba(NH_3)_7C_{60}{\cdot}NH_3$[14] and similar phases). This prevents the definitive identification of ND_3 orientations associated with a specific $Na(ND_3)_2$ complex, with Figure 3a representing the most chemically sensible local description. More complex models, with multiple ND_3 orientations, were tested but could not be converged satisfactorily. A model involving

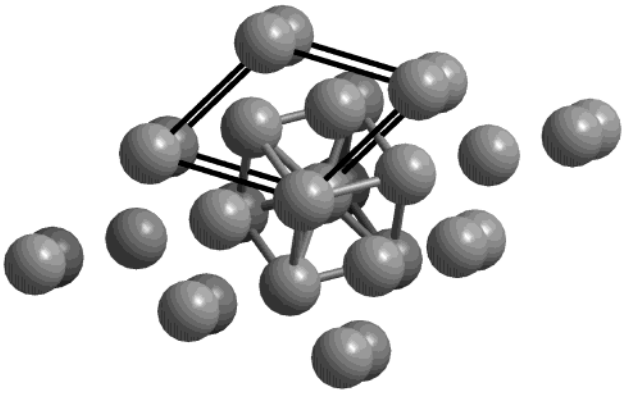

Figure 4. Relationship between the sodium site-disordered $(ND_3)_6Na_2C_{60}$ (cube delineated by gray solid lines) and sodium site-ordered $(NH_3)_{5.3}Na_2C_{60}$ unit cell (black lines), viewed close to the [001] direction of the trigonal $(NH_3)_{5.3}Na_2C_{60}$ cell. Fulleride anions in the pseudo-bcc array are represented as spheres and the eight nearest neighbors in the bcc cell are connected by gray solid lines.

disorder of the ND_3 units over the vertexes of a cube converged to $\chi^2 = 3.8$, indicating that the observed orientational disorder of the ND_3 units does not correspond to rotational diffusion. The network of Na...N contacts is shown in Figure 3b.

$(NH_3)_{5.3}Na_2C_{60}$ adopts a trigonal structure which is derived from a rhombohedral distortion ($c/a = 0.609$) of $(ND_3)_6Na_2C_{60}$ ($c_{trig}/a_{trig} = 0.6124$ for the undistorted bcc cell) (Figure 4). This corresponds to compressing the bcc unit cell along the ⟨111⟩ direction. The diffraction pattern shows no systematic absences, and so given the clear structural relationship to $(ND_3)_6Na_2C_{60}$ further analysis was conducted in $P\bar{3}$ which is the only centric trigonal group which can be derived from maximal nonisomorphic subgroups of $Im\bar{3}$. Initial models were constructed by refining the data in $Im\bar{3}$ using the Na and N positions found in the disordered $(ND_3)_6Na_2C_{60}$ structure above, followed by reduction of symmetry to $P\bar{3}$. Neutral atom scattering factors were used for Na and C, NH_3 was approximated by 1.42 times the scattering factor for nitrogen to allow for the electron density due to the protons. This corresponds to assigning the symmetry lowering from cubic to trigonal to the ordered occupancy of the disordered metal and ammonia sites in the cubic space group. Refinement of this model yields some order of the sodium and nitrogen sites. However, the resultant model was not physically reasonable because the Na−Na and N−N nonbonded contacts are too short given the resulting occupancies. We therefore concluded that the data did not allow a unique and physically acceptable refinement of this highly disordered system by this approach, and the absence of diffraction data at high angle defeated efforts to use conventional Fourier methods to resolve the disorder.

Therefore, this model was used as a starting point for REMEDY[15,16] cycles using a combination of RIETAN-2000 and the MEED/MEVIUS programs developed by Sakata and co-workers.[9] Initially F_{obs} were

(14) Himmel, K.; Jansen, M. *Inorg. Chem.* **1998**, *37*, 3437−3439.

(15) Izumi, F.; Yamamoto, A.; Khasanova, N. R.; Kumazawa, S.; Hu, W. Z.; Kamiyama, T. *Physica C* **2000**, *335*, 239−244.

(16) Kumazawa, S.; Yamamura, S.; Nishibori, E.; Takata, M.; Sakata, M.; Izumi, F.; Ishii, Y. *J. Phys. Chem. Solids* **1999**, *60*, 1407−1409.

extracted on the basis of the model described in the previous paragraph. These values were then used to calculate an electron density map, using the method first employed by Collins[7] as implemented by Sakata and co-workers.[9,10] The electron density in the unit cell is divided into a number of voxels (in this case 64 × 64 × 64) and the electron density refined against F_{obs} starting from an initial featureless map. The resulting density map is used to calculate a set of F_{calc} values which are used to extract a further set of F_{obs}. The process is repeated in order to remove the bias of the initial model. No further improvement in the fit was obtained after 4 cycles ($R(F^2)$ improved from 9.58% to 2.05%, as shown in Figure 5a). The electron density map thus generated clearly showed the different setting angles of the symmetry-independent sets of fulleride anions (Figure 5b) and allowed the location of five sites not associated with the C_{60} anions, all of which were general positions (*6g*). Two of these sites were in close proximity (<2 Å), and were thus refined as being partially occupied (with the sum of the occupancies fixed at 1.42, which approximates to 1 NH_3, vide supra). Given the identical electron counts of the Na^+ and NH_3 units, assignment of the site occupancy to chemical species was made using chemical bonding and coordination number considerations. The sodium was chosen to be on the site with the most reasonable distances to carbon (Figure 5c), which is also coordinated by two of the other non-C_{60} sites. The remaining sites were assumed to be fully occupied by NH_3, leading to a final refined composition of $(NH_3)_{5.73(4)}Na_2C_{60}$. Given the disorder present in the material, this is acceptably close to the composition determined from the ammonia sorption isotherm.

An important feature of the symmetry lowering from cubic to trigonal is that two crystallographically inequivalent C_{60}^{2-} sites are present: one is located at the *1a* position (0,0,0; site symmetry $\bar{3}$) and the second is located on *2d* ($^1/_3$, $^2/_3$, *z*; $z \sim {}^2/_3$, site symmetry 3). Because of the absence of diffraction at high angle, both of these anions were modeled as rigid bodies with only the rotation angle of each anion around the 3-fold axis and the *z* displacement of the *2d* anion refined. Initial orientations for the C_{60}^{2-} anions were obtained from the MEED map, and the setting angles were then refined to values close to these initial ones. Final Rietveld fits, which employed an overall thermal parameter, are shown in Figure 6a, and the resulting C_{60} orientations are shown in Figure 6b. The refined parameters are given in Table 3, and the resulting bond lengths and angles are provided in Table 4.

$(NH_3)_{5.3}Na_2C_{60}$ gives a single peak in the room temperature ^{13}C MAS spectrum at 184 ppm, compared to the shift of 172 ppm found for Na_2C_{60}[17] (Figure 7). The full width at half-height is 115 Hz, compared with the value of 28 Hz found for the Na_2C_{60} starting material. This considerable enhancement in the breadth of the ^{13}C MAS NMR resonance is consistent with the development of two similar but distinct C_{60} sites as required by the space group symmetry.

The sodium is unsymmetrically bound by the fully occupied NH_3b site at 2.23(3) Å and the approximately half occupied NH_3c and NH_3d sites at 3.04(7) and 2.82(8) Å, respectively. The sodium site is approximately equidistant between two 6:6 ring junctions of the two different C_{60} sites (Figure 8). Figure 8b,c shows a comparison of location of the sodium site relative to the six sites generated by symmetry lowering from the positionally disordered $Im\bar{3}$ phase. The distances between the occupied site in the ordered phase and the parent disordered sites vary between 4.334 and 1.485 Å, with the two closest sites at 1.485 and 1.701 Å. The sodium cation has moved from the centroid of these sites to a position between the two C_{60}^{2-} anions which coordinate to it.

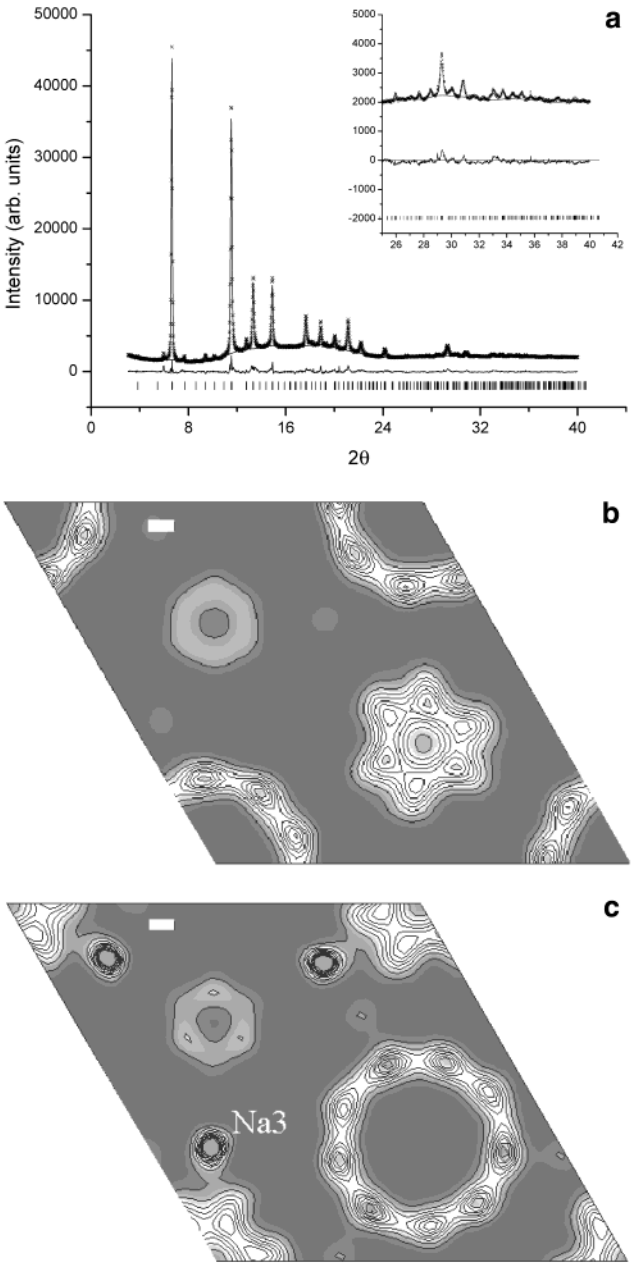

Figure 5. (a) REMEDY fit to the diffraction pattern of $(NH_3)_{5.3}Na_2C_{60}$. (b) Sections of the **ab** plane at $z = 0.05$ of the MEED/REMEDY electron density of $(NH_3)_{5.3}Na_2C_{60}$ showing the orientation of the C_{60} on the *2b* position (contours are marked at 0.3 eÅ^{-3}, scale bar is 1 Å). (c) Sections of the **ab** plane at $z = 0.28$ of the MEED/REMEDY electron density of $(NH_3)_{5.3}Na_2C_{60}$ showing the location of the Na3 site (contours are marked at 0.3 eÅ^{-3}, scale bar is 1 Å).

(17) Douthwaite, R. E.; Green, M. L. H.; Rosseinsky, M. J. *Chem. Mater.* **1996**, *8*, 394−400.

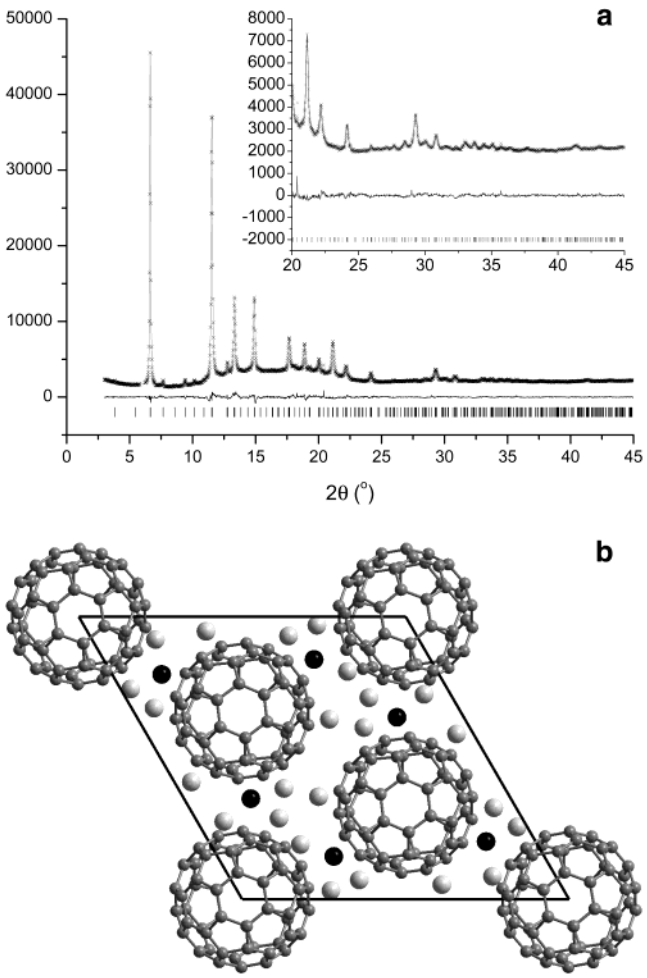

Figure 6. (a) Rietveld fit to synchrotron X-ray powder diffraction data from $(ND_3)_{5.3}Na_2C_{60}$. The observed data are shown as points, the calculated fit is the solid line, and the difference is plotted below. The tick marks indicate the location of the Bragg peaks ($\chi^2 = 3.65$, $R_{wp} = 2.83\%$ $R_p = 2.29\%$, $R(F^2) = 6.48\%$.) Space group $P\bar{3}$ (no. 147) $a = 17.227(1)$ Å, $c = 10.500(1)$ Å, $V = 2698.9(5)$ Å^3. The refined parameters are given in Table 3 and the lengths are provided in Table 4. (b) Refined setting angles of the two independent C_{60}^{2-} anions, viewed along [001]. Na cations are represented as black and NH_3 molecules are shown as light spheres.

The ordering of the sodium positions is coupled crystallographically to the development of the two distinct fulleride environments. The occupied sodium sites form an octahedron around the C_{60} on site *1a* (the Na sites are 6.101 Å from the anion centroid). The other C_{60} site (*2d*), which relaxes by 0.355(3) Å along *c* toward the *1a* site, also has six Na nearest neighbors. However, the sodium sites are now arranged in a distorted trigonal prism. There are three short Na-centroid distances (6.381 Å) forming one triangular face of the trigonal prism, and three long distances (7.705 Å). The arrangements of the sodiums and ammonias around the two different C_{60} sites are shown in Figure 9. The mean Na−C_{60} distance is considerably longer to the *2d* C_{60}, consistent with different anion charges. (Assuming that the interactions between the Na^+ and C_{60} anions are purely electrostatic, the distances between the C_{60} centroids and the cations will depend on the relative charges on the C_{60} anions, and based on this simple estimate a 15% charge difference is indicated.) This is the first example of the development of two different

Table 3. Refined Parameters for $Na_2(NH_3)_{5.3}C_{60}$[a]

	x	*y*	*z*	fractional occupancy
C1a	0.17396(28)	0.1038(21)	0.2324300	1
C2a	0.2217(12)	0.0408(34)	0.0548110	1
C3a	0.09501(24)	0.0618(11)	0.3120690	1
C4a	0.1913(14)	0.1789(17)	0.1549790	1
C5a	0.1906(10)	0.0347(29)	0.1826350	1
C6a	0.0342(13)	0.09512(23)	0.3133760	1
C7a	0.1265(25)	0.2097(4)	0.1529670	1
C8a	0.0508(24)	0.1693(6)	0.2294000	1
C9a	0.1223(30)	0.23948(4)	0.0242370	1
C10a	0.2229(12)	0.1848(22)	0.0248410	1
C1b	0.54143(34)	0.7399(19)	0.5398(8)	1
C2b	0.12527(34)	0.5934(19)	0.8457(8)	1
C3b	0.2743(16)	0.49561(30)	0.4634(8)	1
C4b	0.16232(30)	0.5546(13)	0.9221(8)	1
C5b	0.2762(8)	0.7055(9)	0.3794(8)	1
C6b	0.3904(7)	0.6279(9)	0.1.0062(8)	1
C7b	0.2269(21)	0.7991(19)	0.6685(8)	1
C8b	0.4398(21)	0.5342(19)	0.7170(8)	1
C9b	0.3087(19)	0.8288(12)	0.8754(8)	1
C10b	0.1465(8)	0.6421(19)	0.5102(8)	1
C11b	0.1607(12)	0.6898(21)	0.8478(8)	1
C12b	0.3565(21)	0.8625(8)	0.5377(8)	1
C13b	0.3912(7)	0.6288(9)	0.3806(8)	1
C14b	0.2755(7)	0.7045(9)	1.0049(8)	1
C15b	0.1563(15)	0.7166(23)	0.7176(8)	1
C16b	0.5104(15)	0.6167(23)	0.6679(8)	1
C17b	0.5508(9)	0.6957(23)	0.7475(8)	1
C18b	0.1159(9)	0.6376(23)	0.6380(8)	1
C19b	0.2368(14)	0.7449(15)	0.9252(8)	1
C20b	0.4116(15)	0.84131(10)	0.4603(8)	1
Na3	0.2044(11)	0.3560(15)	0.2824(19)	1
NH_3a	0.0519(21)	0.4151(21)	0.2101(31)	1.35(2)
NH_3b	0.3238(18)	0.3923(19)	0.1597(31)	1.29(3)
NH_3c	0.194(4)	−0.081(5)	0.510(6)	0.64(4)
NH_3d	0.287(4)	0.031(5)	0.511(7)	0.78(4)

[a] All the atoms occupy the *6 g* positions. The NH_3 groups were refined using the N form factor, and thus occupancies should be divided by 1.42 to yield the fractional occupancy of NH_3, as discussed in the text. The C_{60} anions were refined as rigid bodies using two parameters for the C_{60} on the *2d* site (translation along c and rotation around the 3-fold axis) and one parameter for the C_{60} on the *1a* site (rotation around the 3-fold axis).

Table 4. Refined Bond Lengths (Å) and Angles (°) in $(NH_3)_{5.3}Na_2C_{60}$

Na3−C7a	2.57(2)
Na3−C8a	3.02(3)
Na3−C3b	2.82(2)
Na3−C1b	3.25(3)
Na3−NH_3b	2.23(2)
Na3−NH_3c	3.04(7)
Na3−NH_3d	2.82(8)
C8a−Na3−C3b	169.3(33)
C8a−Na3−NH_3d	85.8(26)
C3b−Na3−NH_3d	102.(4)

anion sites in a fulleride in which the anions are in electronic contact, and may indicate an uneven distribution of the t_{1u} electrons between the distinct anions, producing a real-space charge-ordered state. This is also reflected in the C_{60}−C_{60} closest contacts. The C_{60} (*1a*) is surrounded by a regular bicapped octahedron of C_{60}'s (2×10.497 Å to *1a* and 6×10.443 Å to *2d*), whereas the C_{60}−C_{60} closest contacts around the *2d* site are significantly distorted (3×10.443 Å to *1a* and 2×10.497 Å, 3×10.782 Å to *2d*).

The three nitrogen sites shift significantly less than the sodium sites when compared with the disordered parent material, and the reduced displacement of these neutral species is further evidence of coupling of the cation positional and anion charge ordering. The non-

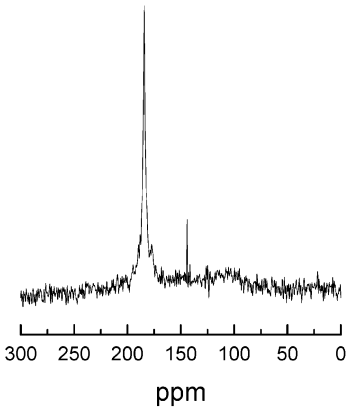

Figure 7. ^{13}C MAS NMR of $(NH_3)_{5.3}Na_2C_{60}$. (The sample on which NMR data were recorded was a larger preparation than that used for diffraction data collection and thus contained a small amount of unreacted C_{60} evident as a sharp line at 143 ppm.)

coordinated NH_3a moves 0.824 Å toward the center of the pseudo-tetrahedral cavity at $^1/_2$, 0, $^1/_4$ and the coordinated NH_3b moves 0.557 Å toward the occupied Na site. The remaining site splits and both components move toward the two adjacent sodium sites (by 1.521 and 0.418 Å). The presence of ammonia not coordinated to sodium in this site-ordered phase indicates the favorable nature of this site in a bcc fulleride array, and gives support to the inference of such noncoordinating ammonia in the site-disordered $(ND_3)_6Na_2C_{60}$ phase.

Discussion

Both phases discussed here are derived from a body-centered packing of the fulleride anions. The reactivity with ammonia of fcc Na_2C_{60}, in which the sodium cations are ordered on the tetrahedral sites, is driven by the need to coordinate all of the small sodium cations to ammonia, which favors more expanded bcc-based structures to allow the $Na(NH_3)_x$ complexes to form. In contrast, the fcc phases Na_2CsC_{60} and K_3C_{60} afford $(NH_3)_4Na_2CsC_{60}$[18] and $(NH_3)K_3C_{60}$[19] with $(NH_3)_4Na^+$ and $[K-NH_3]^+$ units on the octahedral sites, while the tetrahedral sites are occupied by uncomplexed cations. The bcc array contains large quasi-tetrahedral interstitial sites which are occupied by the cations in K_6C_{60}.[20] Although neutral fcc-packed C_{60} does not take up ammonia, these large interstitial sites in the bcc array are favorable locations for the ammonia molecules and are occupied in both the phases discussed here. The site allows C...D nonbonded contacts within the range normally associated with N−D...π interactions, which accounts for its occupation by ND_3 even when the molecule does not coordinate to a cation. However, although the fully occupied ND_3 site in the disordered $(ND_3)_6Na_2C_{60}$ material (formed by desorption from $(ND_3)_8Na_2C_{60}$) remains in a similar position in $(NH_3)_{5.3}$-Na_2C_{60}, the subtle change in the number of ND_3 molecules sorbed by Na_2C_{60} in the two samples, which may reflect the different preparative methods used

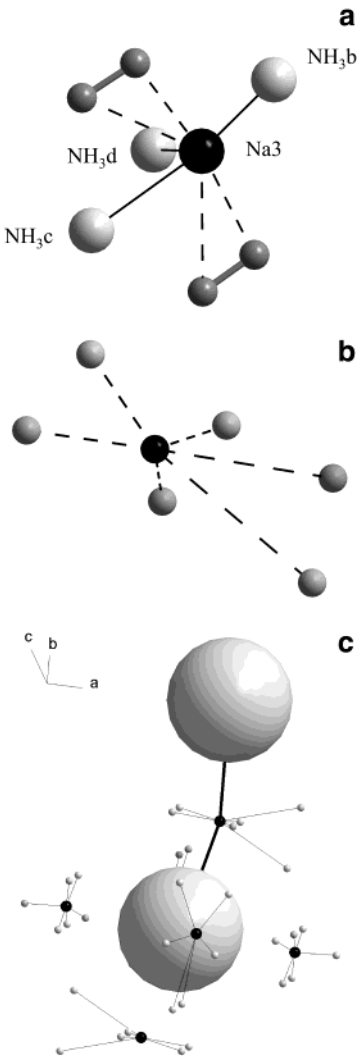

Figure 8. (a) Sodium site in $(NH_3)_{5.3}Na(C_{60})$. The sodium cations are shown as black spheres, the N atoms of the NH_3 molecules are light gray, and the carbon atoms are medium gray spheres. (b) Comparison of the location of the refined, fully occupied sodium site (black sphere) in $(NH_3)_{5.3}Na_2C_{60}$ with the disordered $^1/_6$ occupied sodium sites (small gray spheres) from the parent $(ND_3)_6Na_2C_{60}$. (c) Indicates the location of the occupied Na site shown in (b) in the unit cell relative to the C_{60} anion (large sphere) on the *1a* position. The disordered sodium sites from the $Im\bar{3}$ parent structure surrounding each occupied site are represented as light gray spheres. Bold lines connect the Na cation in (b) to its C_{60} neighbors.

(significant hysteresis is observed in room-temperature isotherm measurements of NH_3 uptake by Na_2C_{60}) leads to dramatic differences in the cation site occupancy and fulleride anion orientational ordering. As the disordered $Na_2(ND_3)_6C_{60}$ is closely related to previously well-studied examples, the discussion below focuses on the new positionally ordered phase.

The major change in the structure of the ordered phase is that instead of the sodium cations occupying a range of sites with 16% probability, one set of these sites is selected for complete occupancy. The ordering of the sodium positions results in retention of only one of the cubic 3-fold axes, and hence drives the lowering of symmetry from cubic to trigonal. The resulting cell can be derived initially by descending in symmetry to rhombohedral, which generates a cell containing three crystallographically equivalent fulleride anions. How-

(18) Zhou, O.; Fleming, R. M.; Murphy, D. W.; Rosseinsky, M. J.; Dover, R. B. v.; Ramirez, A. P.; Haddon, R. C. *Nature* **1993**, *362*, 433.
(19) Rosseinsky, M. J.; Murphy, D. W.; Fleming, R. M.; Zhou, O. *Nature* **1993**, *364*, 425−427.
(20) Zhou, O.; Cox, D. E. *J. Phys. Chem. Solids* **1992**, *53*, 1373.

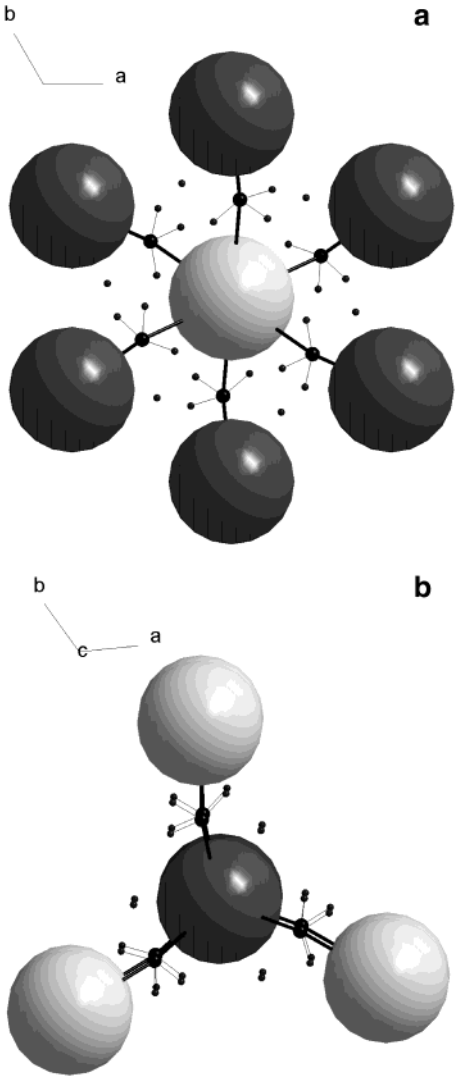

Figure 9. (a) Arrangement of sodium (black spheres) and nitrogen (medium-sized spheres) around the C_{60} anions at the *1a* sites (large light gray spheres), viewed along the 3-fold axis. (b) Arrangement of sodium and nitrogen around the C_{60} anions at the *2d* sites (large dark gray spheres), viewed along the 3-fold axis. The shorter sodium-centroid distances are directed out of the page.

ever, the cation site ordering requires the loss of the rhombohedral centring translations and results in the development of two distinct fulleride anion sites within the now trigonal cell. The cation site ordering and anion site inequivalence are coupled together in an interesting and potentially significant way. The sodium−C_{60} distances indicate that this differentiation is associated with the development of slightly different charges on the fulleride anions, which also differ in their rotational setting angles about the trigonal [001] direction. The broadening of the ^{13}C MAS NMR resonance compared with the Na_2C_{60} parent phase is consistent with a more heterogeneous charge distribution over the carbon atoms in the $(NH_3)_{5.3}Na_2C_{60}$ phase, although the broadening can also be partially ascribed to $^{13}C-^{1}H$ dipolar coupling.

The indications of similarities between these materials and the highly correlated transition metal oxide systems are strong. The observation of an electronically interacting array of fulleride anions with crystallographically distinguishable components is significant given the importance of real-space valency ordering in determining the properties of the transition metal oxides, which are archetypal examples of strongly correlated electronic systems. Charge-ordering in oxides is associated with electron localization and insulating behavior.[21] The fullerides are also narrow band systems, as the on-site interelectron repulsion U is comparable to the t_{1u} bandwidth W, with estimates of U/W placing the A_3C_{60} systems in the localized regime of conventional singly degenerate Mott−Hubbard models. However, in cubic A_3C_{60} systems, the t_{1u} orbital degeneracy stabilizes the metallic states by opening up alternative hopping channels.[22] Loss of the t_{1u} degeneracy by symmetry lowering stabilizes magnetic insulating ground states in orthorhombic fullerides[2,3] with the same anion density as metallic cubic phases.[23] In the present case, the interanion separations are similar to those found in magnetic insulating noncubic fullerides. $(ND_3)_{5.3}Na_2C_{60}$, however, differs from the previous expanded low-symmetry fullerides in that its structure results from ordering of the charge-compensating sodium cations. This ordering occurs to generate two quite distinct fulleride anion environments, suggesting that it is coupled with localization of the t_{1u} electrons on the distinct anion sites in an inhomogeneous manner, producing the first example of a charge-ordered fulleride. This is supported by the breadth of the ^{13}C MAS NMR resonance and the distinct interfulleride contacts at the two sites.

Acknowledgment. We thank the EPSRC for support under GR/M 04006 and the Leverhulme Trust for support under F/25/BX. M. A. Roberts and S. Hull provided expert experimental assistance on the 9.1 and POLARIS diffractometers.

Supporting Information Available: ORTEP and other graphical representations of the structures of the studied compounds (PDF). This material is available free of charge via the Internet at http://pubs.acs.org.

CM020161X

(21) Rao, C. N. R.; Arulraj, A.; Cheetham, A. K.; Raveau, B. *J. Phys. Condens. Matter* **2000**, *12*, 83−106.
(22) Gunnarsson, O.; Koch, E.; Martin, R. M. *Phys. Rev. B* **1997**, *56*, 1146.
(23) Dahlke, P.; Denning, M. S.; Henry, P. F.; Rosseinsky, M. J. *J. Am. Chem. Soc* **2000**, *122*, 12352−12361.